Proceedings of BALTTRIB'2022 edited by prof. J. Padgurskas
eISSN 2424-5089 (Online)
DOI: 10.15544/balttrib.2022.11

VISCOSITY MODELS OF C60 FULLERENE MINERAL OILS AND COMPUTATIONAL FLUID DYNAMICS ON PISTON RING

E. Tsakiridis, P.G. Nikolakopoulos*
Mechanical Engineering and Aeronautics Department, University of Patras, Greece

Abstract. To improve even more the efficiency in automotive engines, it is crucial to fully understand the generation of friction in its components. In recent years the usage of mineral and synthetic or semi-synthetic oils has increased. Nowadays worldwide massive research over nanoparticles and as a result nanolubricants has taken place. Results of research under laboratory conditions on the aging of engine commercial oils with different performance levels (such as mineral SAE 30, synthetic SAE 10W40) are presented in this paper. It is described that the action of pressure and temperature play a key role of the engine oils behaviour. The aging of lubricant causes changes to its dynamic viscosity. In this work an investigation was carried out using CFD simulations and piston ring-cylinder problem. The friction as well as the absolute pressure has been measured for all the crankshaft angles. The thermal problem has also been solved due to the fact that temperature variations affects on the oil viscosity. The temperature and the piston ring velocity varied according to the angle of the crankshaft.

Keywords. Lubricants, fullerene C60, ageing, viscosity measurements.

1. INTRODUCTION

Synthetic lubricants are often including nanoparticles as additives. These nanoparticles have different size, shape, and volumetric concentration. For many tribological applications, the lubricants with nanoparticles have shown better performance in friction and wear, owing to high dispersion properties, improved lubricant properties and thermal transfer. Therefore, an understanding of nanoparticles, like fullerenes C60, behavior is necessary to improve lubrication mechanisms, which in practice might help in complying to stringent vehicle emission regulations. In 2015, Spikes [1] referred that the importance of tribofilm formation from friction modifiers and anti−wear additives within the contact is continuously increasing. Particularly, a beneficial effect on frictional and energy losses can be addressed on transportation section. This strategy has experienced in the mixed and boundary regimes of lubrication, where the oil film is limited [2]. Several types of nanoparticles with sizes in the range 1–120 nm was added to different lubricants in order to achieve lower friction and wear for various contacts. Lee et al. [3] reported the impact of fullerene nanoparticles using a disk-on-disk tribometer. They showed that synthetic lubricant could result in higher friction reduction of 90% in comparison the base oil. Padgurskas et al. [4] investigated the effect of Fe, Cu and Co nanoparticles and their combinations in a mineral oil. They found that Cu nanoparticles are more effective than others, reducing the friction and wear. Wan et al. [5] also showed the main properties of lubricant oil including boron nitride nanoparticles. They used different concentration of nanoparticles in a commercial oil SAE 15W40. It was indicated that optimal size and concentration of particles should be 120 nm and 0.1 wt % accordingly. This consideration showed a friction reduction by 77% in comparison with base oil.

To demonstrate the basic lubrication mechanisms in the piston ring conjunction, advanced models were developed in recent years from many tribologists. Because of the transient engine conditions, rapid loads and engine velocity would result in different contact conditions. Boundary/mixed and hydrodynamic regimes are main lubrication stages as the ring reciprocates from Top Dead Center to Bottom Dead Center.

* Author for contacts: Prof. P. G. Nikolakopoulos
E–mail: pnikolakop@upatras.gr

Thus, generated ring friction is highly sensitive to Poiseuille shear and direct contact of asperities. Under these conditions, lubricants containing nanoparticles protect the counter face surfaces reducing contact wear and improve oil degradation.

In the context of this research, a 2D Computational Fluid Dynamics (CFD) model was developed based on Navier-Stokes equation, vapor transport, Lagrangian approach for nanoparticles motion, and the following configurations: i) The studied piston ring is taken from a motorbike engine, with an ideal parabolic ring profile. Full lubrication (a–b), cavitation (b–c) and lubricant reformation (c–d) are the basic lubrication regions ii) The flow is laminar, and the lubricant properties are changed according to pressure and temperature into the contact. iii)Two phase flow is included using vapour transport approach (Rayleigh–Plesset equation) with no artificial boundary conditions iv) Lagrangian method is used to solve the equations for the nanoparticles, as well as a large number of particles are moved individually through the lubricant field. v) Under mixed conditions, the load of asperities is taken into account using the stochastic model of Greenwood-Tripp.

2. THEORY AND MODELING

A 2D CFD model is built using the Ansys FLUENT. The flow problem is nonlinear, and the governing equations are coupled together. The pressure-based mixture model is used, while the velocity–pressure coupling was treated using the Semi-implicit Method for Pressure-linked Equations (SIMPLE) algorithm. The SIMPLE algorithm reduces the discretisation-induced errors in the calculations including second-order upwind configuration. Grid sensitivity tests are obtained to find better mesh requirements. A total number of 31.031 quadrilateral volumes are considered in this case. Furthermore, the time step is taken as 10^{-3} s. This configuration is determined for flow stabilization during the simulation. Convergence criterion of 10^{-5} was taken into account. The power-law model was used for viscosity, Zavos and Nikolakopoulos [25].

The ring moved along the cylinder inner liner according to the piston sliding velocity. This velocity is calculated as [20]:

$$u_{ring} \approx v_p = r_{cr}\omega(\sin\varphi + \frac{\lambda_{cr}}{2}\sin 2\varphi) \tag{1}$$

where r is the crank-pin radius, ω is the rotational engine speed, φ is the crank angle and λ_{CR} is the control ratio. Ring twist is not considered. The lubricant film thickness between the ring and the liner can be approximated as the following:

$$h(x,y,t) = h_{\min}(t) + h_s(x) + \delta(x,y,t) \tag{2}$$

where $h_{\min}(t)$ is the minimum lubricant film, $h_s(x)$ is the parabolic ring profile and δ is the localized contact pressure-induced deflection. The final parameter has a limited effect for this analysis.

Calculated the gas pressure behind the ring, the main forces are illustrated in Figure 3 and rewritten here. The back-gas force is obtained as:

$$F_G = \pi d_{cyl} b p_{bk}(\varphi) \tag{3}$$

and the ring tension force is also defined as:

$$F_{el} = \pi d_{cyl} b p_{el} \tag{4}$$

where the elastic pressure is expressed as:

$$p_{el} = \frac{d_{gap} E_r \frac{bd^3}{12}}{3\pi b\left(\frac{d_{cyl}}{2}\right)^4} \tag{5}$$

where d_{gap} is the piston-ring end gap and d_{cyl} is the cylinder bore diameter.

The mechanism of mixed lubrication has a critical impact in piston ring conjunction owing to rapidly changing running engine conditions. This is obvious as the ring moved near to dead centers where the speed is low and contact load is predominant. In the current analysis, the stochastic model of Greenwood-Tripp [16] is used to predict the load of asperities and contact area accordingly. Greenwood and Tripp's approach for two nominally flat, rough surfaces is a conventional model to express asperities impact in ring-liner contact. However, statistical contact models are more useful predicting with better accuracy the ring and cylinder surfaces [30]. Many works have tried to study the changes of surface topography during running-in of the engine whose surfaces are non-Gaussian.Thus, a more comprehensive contact model for both Gaussian and non-Gaussian surfaces should be addressed. This issue remains the motivation for further improvement of the proposed model.

Assuming that the asperity height distribution is Gaussian, the generated contact pressure can be defined as:

$$p_c = \frac{W_c}{A_c} \tag{6}$$

where $W_c = \frac{16\sqrt{2}}{15}\pi\left(\zeta\kappa\sigma\right)^2\sqrt{\frac{\sigma}{\kappa}}E' AF_{5/2}\left(\lambda\right)$ is the load carried by the asperities and $A_c = \pi^2\left(\zeta\kappa\sigma\right)^2 AF_2\left(\lambda\right)$ is the corresponding contact area.

The probability distribution of asperity heights $F_{5/2}(\lambda),F_2(\lambda)$ is analysed by a fifth-order polynomial curve [18].

Analysis of nanoparticles motion.

To simulate the nanoparticles motion into the fluid, small and spherical particles are considered to this case. Particularly, the Basset–Boussinesq–Oseen expression (BBO equation) is used throughout the Ansys FLUENT code. The governing equation is given as [15]:

$$\frac{\pi}{6}\rho_p d_p^3\frac{d\overrightarrow{V_p}}{dt} = 3\pi\mu d_p\left(\vec{V}-\overrightarrow{V_p}\right) - \frac{\cdots}{6}d_p^3\nabla p + \frac{\cdots}{12}\rho d_p^3\frac{\cdots}{dt}\left(\vec{V}-\overrightarrow{V_p}\right) + \frac{\cdots}{2}d_p^2\sqrt{\pi\rho_f\mu}\int_{t_o}\frac{\cdots}{\sqrt{t-\tau}}\frac{\cdots}{d\tau}\left(\vec{V}-\overrightarrow{V_p}\right)d\tau + \sum_{\kappa}\overrightarrow{F_\kappa} \tag{7}$$

This mathematical formula promotes the trajectory of each particles during the lubricant motion. In more details, this is Newton's second law, in which the left-hand side is the rate of change of the particle's linear momentum, and the right-hand side is the contribution of the viscous, gravitational, buoyancy, virtual mass, and Basset forces acting on the nanoparticle. The basic terms on the right side are defined as:

- Stokes' drag,
- Froude–Krylov force due to the pressure gradient in the lubricant flow. Note that the pressure gradient estimated from Navier-Stokes equation as follows:

$$-\nabla p = \rho\frac{D\vec{V}}{Dt} - \mu\nabla^2\vec{V} \tag{8}$$

- the unsteady force due to the added mass effect,
- Basset force and other forces acting on the particle, such as the effects of Brownian motion. This trend is not taken into account owing to the size of nanoparticles. In this case, the sizes of nanoparticles are 100 nm.

The effective lubricant viscosity is modelled as a relationship of pressure and temperature by the Houpert investigation [19]:

$$\mu = \mu_o \exp\left\{(\ln \mu_o + 9.67)\left[\left(\frac{\theta_{av} - 138}{\theta_o - 138}\right)^{-S_o}\left(1 + \frac{p_{hyd} - p_{atm}}{1.98 \times 10^8}\right)^{Z_o} - 1\right]\right\} \quad (9)$$

where the parameters S_o and Z_o are determined by Gohar and Rahnejat [20].

Simulations were performed and compared to the experimental data, reported previously. During those tests, a four-stroke motorbike engine operated at idle speed of 1000 min^{-1}.

After using the boundary and load conditions of a previous paper [8, 10, 14, 18, 24, 25] published several years ago for the simulation it was observed that the simulation results are matching those established experimentally.

First of all, the minimum film thickness is calculated from the simulations and shown in Figure 1. As it is observed the lubricant 10W30 corresponds to a higher minimum film thickness while the fullerenes lubricants correspond respectively in lower film thicknesses. It is observed in all phases of the combustion. This is due to the fact that the lubricant with fullerenes as additives has lower viscosity and retains its properties, as does 10W30 lubricant, under all operating conditions.

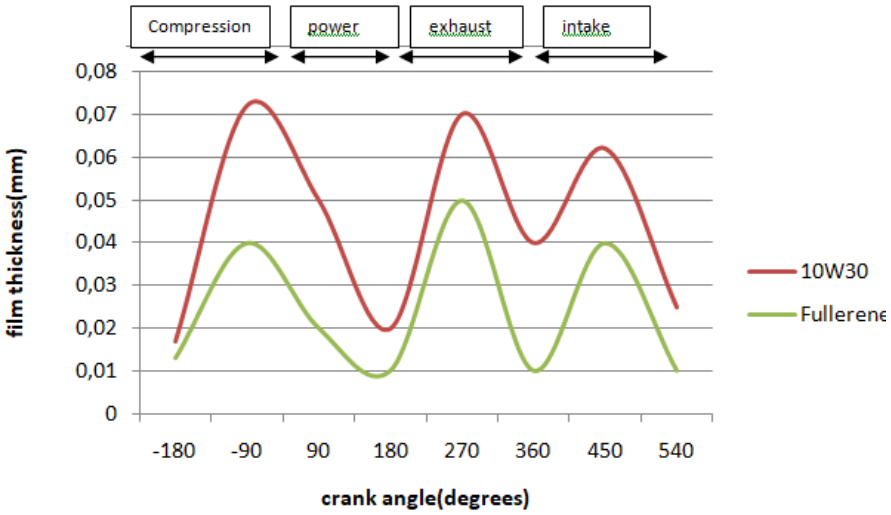

Figure 1. The minimum film thickness at 398 K.

At each crank angle for the minimum lubricant film thickness the maximum hydrodynamic pressure is shown in the figure 2.

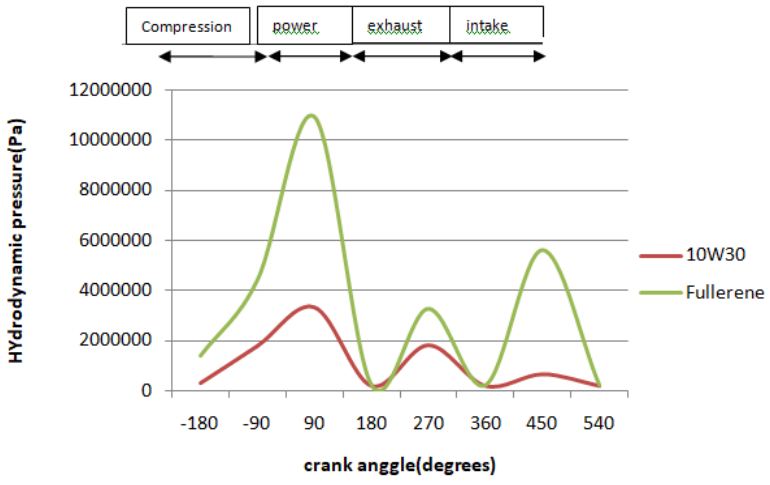

Figure 2. The maximum hydrodynamic pressure at 398 K.

As expected, the pressure is bigger if the film thickness is lower. And so the pressure, if the lubricant with C60 fullerenes as additives is used, is much higher. But the viscous friction, which causes wear and decreases the performance of the engine, has extreme differential between the two lubricants. This happens because the viscous fiction depends on viscosity, which is much lower for fullerenes lubricant.

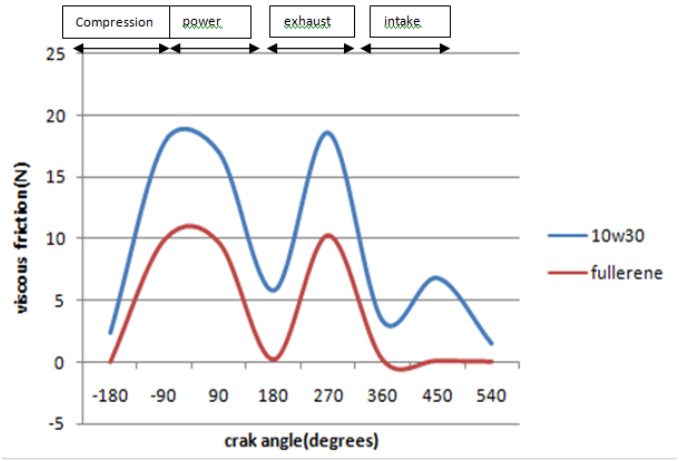

Figure 3. Viscous friction at 398 K.

The temperature through the flow is changing and that change is what the following figure shows. As it is expected the differential is observed near the piston ring which has heat flux and so the temperature varies in the area next to it. The temperature of the cylinder is considered as 398 K.

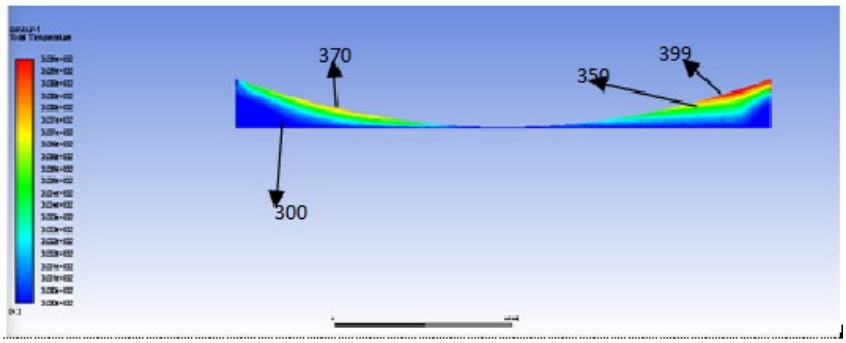

Figure 4. Temperature distribution through lubricant 10W40.

If the lubricant with fullerenes additives is used the temperature distribution is shown in figure 5. It is obtained that the temperature is similar through the lubricants, but the distribution is lower in the case of fullerenes lubricants, which causes the stability of its viscosity and its properties in general. This happens due to fullerenes thermal properties.

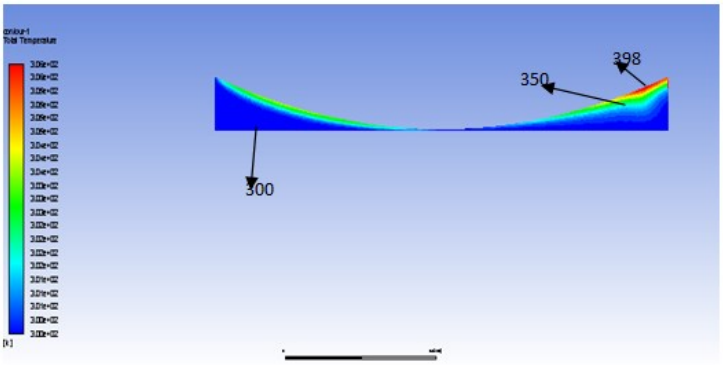

Figure 5. Temperature distribution for lubricant with fullerenes.

All these results are according to Harigaya et al. (6). After using just the same inputs and boundary conditions, the results taken could be told that are the same.

This assumption has great application in piston ring-liner tribo-system from different researchers showing good predictions with experimental data. Zavos et al. [10], Gore et al. [22] and Söderfjäll et al. [23] focused recently on the piston ring conjunction including numerical predictions and direct measurements with well verification. Of course, ring shape and roughness can affect lubrication mechanisms during mixed and hydrodynamic regime. This is obvious to previous work of Zavos and Nikolakopoulos [10], where the difference can be varied between 5–25% depending on the running conditions. Therefore, the effect of lubricant with nanoparticles using an advanced CFD model is the main contribution of this study.

Table 1. Basic parameters for the CFD model in piston ring-liner contact.

Parameters	Values	Units
Ring base material	Steel	–
Coating	Chromium plated	–
Young's modulus of elasticity for ring	270	GPa
Ring Poisson's ratio	0.21	–
Ring face width	0.5	mm
Ring radial width	3.3	mm
Ring end gap	0.2	mm
Ring curvature	3	mm
Ring roughness	0.2	mm
Cylinder base Material	Aluminium	–
Young's modulus of elasticity for ring	70	GPa
Ring Poisson's ratio	0.33	–
Cylinder roughness	0.15	mm
Roughness parameter	0.04	–
Asperity slope	0.0015	–

The viscosity has been measured using an EH105 capillary tube viscometer manufactured by DELTALAB (Carcasonne, France). P. G. Nikolakopoulos et. al [24] have done the same measurements and the results, for a SAE 10W40 fresh and 100 hr aged, are shown in the figure 6 below.

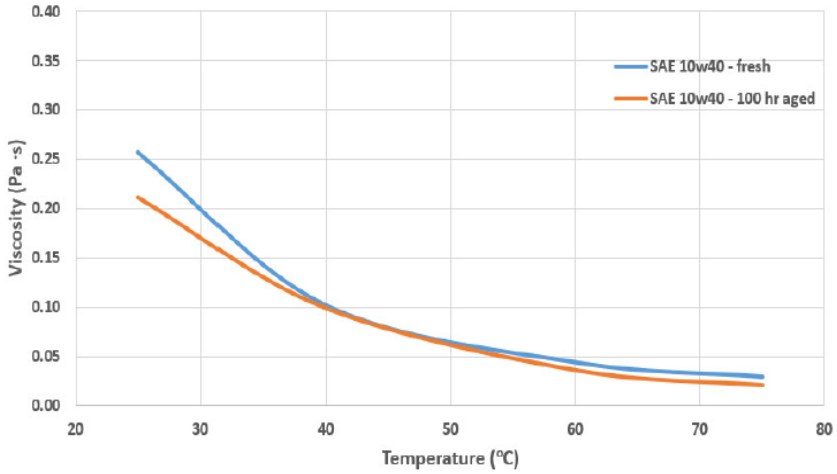

Figure 6. Measured viscosity for fresh and aged synthetic oil SAE 10W40 [24].

CONCLUSIONS

A CFD model is developed in order to study the effect of lubricants contain fullerenes against synthetic oils, on the tribology piston ring problem. It is obtained that the film thickness in fullerenes

lubricants with the highest value might be achieved in 270 degrees of crank angle while the friction is minimum in 180 degrees of crank angle. For example, the maximum variation of the minimum film thickness is about 30% while the maximum variation of friction is about 42%.

REFERENCES

[1] Spikes H. Friction Modifier Additives. Tribol. Lett. 2015, 60.
[2] Rudnick L.S. Lubricant Additives–Chemistry and Applications, 2nd ed.; CRC Press: Boca Raton, FL, USA, 2009.
[3] Lee K., Hwang Y., Cheong S., Kwon L., Kim S., Lee J. Performance evaluation of nano-lubricants of fullerene nanoparticles in refrigeration mineral oil. Current Applied Physics 9(2) (2009), e128–e131.
[4] Padgurskas J., Rukuiza R., Prosyčevas I., Kreivaitis R. Tribological propertiesof lubricant additives of Fe, Cu and Co nanoparticles. Tribology International, 60 (2013), 224–232.
[5] Wan Q., Jin Y., Sun P. Ding Y. Tribological Behaviour of a Lubricant Oil Containing Boron Nitride Nanoparticles. Procedia Engineering, 102 (2015), pp. 1038–1045.
[6] Yasuo Harigaya, Michiyosi Suzuki, Fujio Toda, Masaaki Tagikuchi. Analysis of Oil Film Thickness and Heat Transfer on a Piston Ring of a Diesel Engine: Effect of Lubricant Viscosity. Journal of Engineering for Gas Turbines and Power 128 (2006), 685–693.
[7] Gohar R., Rahnejat H. Fundamentals of tribology. London (UK): Imperial College Press; 2008.
[8] Zavos A., Nikolakopoulos P. Thermo-mixed lubrication analysis of coated compression rings with worn cylinder profiles. Ind Lubr Trib. 69(1), (2017), 15–29.
[9] Baker C., Rahmani R., Karagiannis I. et al. Effect of compression ring elastodynamics behaviour upon blowby and power loss (No. 2014–01–1669). SAE Technical Paper; 2014.
[10] Zavos A., Nikolakopoulos PG. Tribology of new thin compression ring of fired engine under controlled conditions–a combined experimental and numerical study. Trib Int. 128 (2018), 214–230.
[11] White F. Viscous fluid flow. 2nd ed. New York (NY): McGraw–Hill; 1991.
[12] Singhal A. K., Athavale M. M., Li H., Jiang Y. (2002). Mathematical basis and validation of the full cavitation model. J. Fluids Eng., 124(3) (2002), 617–624.
[13] Shahmohamadi H., Rahmani R., Rahnejat H., et al. Thermo-mixed hydrodynamics of piston compression ring conjunction. Trib Lett. 51(3) (2013), 323–340.
[14] Zavos A., Nikolakopoulos P. G. Cavitation effects on textured compression rings in mixed lubrication. Lubrication Science, 28(8) (2016), 475–504.
[15] Zhu Chao, Fan Liang-Shi. Chapter 18 – Multiphase flow: Gas/Solid. In Johnson, Richard W. (ed.). The Handbook of Fluid Dynamics. Springer. 2008. ISBN 9783540646129.
[16] Greenwood JA., Tripp JH. The contact of two nominally flat rough surfaces. Proc Inst Mech Eng. 185 (1970), 625–633.
[17] Leighton M., Morris N., Rahmani R., Rahnejat H. Surface specific asperity model for prediction of friction in boundary and mixed regimes of lubrication. Meccanica, 52(1) (2017), 21–33.
[18] Zavos A., Nikolakopoulos P.G. Computational fluid dynamics analysis of top compression ring in mixed lubrication. Mechanics & Industry 18 (2017), No. 2, 208.
[19] Houpert L. New results of traction force calculations in elastohydrodynamic contacts. J Tribol, 107 (1985), 241–245.
[20] Baker C., Theodossiades S., Rahmani R., Rahnejat H., Fitzsimons B. On the transient three-dimensional tribodynamics of internal combustion engine top compression ring. Journal of Engineering for Gas Turbines and Power, 139(6), (2017).
[21] Tomanik E., Profito F., Sheets B., Souza R. Combined lubricant–surface system approach for potential passenger car CO_2 reduction on piston-ring-cylinder bore assembly. Tribology International, (2018). 105514.
[22] Gore M., Rahmani R., Rahnejat H., et al. Assessment of friction from compression ring conjunction of a highperformance internal combustion engine: a combined numerical and experimental study. Proceed Inst Mech Eng J Mech Eng Sci. 230 (12) (2016), 2073–2085.
[23] Söderfjäll M., Almqvist A., Larsson R. Component test for simulation of piston ring–cylinder liner friction at realistic speeds. Trib Int. 104 (2016), 57–63.
[24] Nikolakopoulos P.G., Mavroudis S., Zavos A. Lubrication performance of engine commercial oils with different performance levels: the effect of engine synthetic oil aging on piston ring tribology under real engine conditions. Lubricants 6(4) (2018), 90.
[25] Zavos A., Nikolakopoulos P.G. A tribological study of piston rings by power law oils. 2016.